LA-UR -86-4066

CONF-861207--6

LA-UR--86-4066

DE87 002889

OSTI

1986

TITLE ATOMISTIC SIMULATIONS OF [001] SYMMETRIC TILT BOUNDARIES IN NI_3Al

AUTHOR(S) S. P. Chen
A. F. Voter
D. J. Srolovitz

SUBMITTED TO The Proceedings of the MRS 1986 Winter Meeting, held in Boston, MA, December 1-5, 1986.

DISCLAIMER

MASTER

Los Alamos Los Alamos National Laboratory
Los Alamos, New Mexico 87545

ATOMISTIC SIMULATIONS OF [001] SYMMETRIC TILT BOUNDARIES IN Ni_3Al

S. P. CHEN, A. F. VOTER, AND D. J. SROLOVITZ
Los Alamos National Laboratory, Los Alamos, NM 87545

ABSTRACT

We report a systematic atomistic simulation study of [001] symmetric tilt grain boundaries (GB) in Ni_3Al, Ni, and Al. We found that the grain boundary energies and cohesive energies of Ni_3Al and pure fcc Ni are approximately the same. Grain boundary energies and cohesive energies in Ni_3Al depends strongly on the grain boundary composition. The Al-rich boundaries have highest grain boundary energies and lowest cohesive energies. This offers an explanation for the stoichiometric effect on the boron ductilization.

INTRODUCTION

The intermetallic compound Ni_3Al, like many other $L1_2$ ordered alloys (Cu_3Au structure), exhibits increasing yield strength with increasing temperatures [1], a very desirable property in high temperature applications. Though Ni_3Al is ductile as a single crystal, it is intergranularly brittle in polycrystalline form [2]. This lack of ductility in the polycrystalline form prohibits the practical application of this material. Recently, Aoki and Izumi [3] were able to produce a substantial increase in the ductility of polycrystalline Ni_3Al by microalloying with small amounts of boron. Liu and coworkers [4] have found that boron increases the ductility only in Ni-rich Ni_3Al samples; the best ductility is achieved in samples with 24 atomic percent Al. Neither the boron effect nor the stoichiometry effect are understood. We report here the results of a systematic study of grain boundaries in Ni_3Al. A preliminary report has been published recently [5].

We have performed a series of computer simulations on symmetric tilt [001] grain boundaries in Ni_3Al using a high quality interatomic potential. The effect of grain boundary composition on the grain boundary energy and the cohesive strength of the grain boundary was studied for nine grain boundaries. The grain boundary composition was found to affect the grain boundary energy by approximately 10%. This finding may help shed some light on the stoichiometry effect mentioned above [4,6]. Also be comparing the grain boundary energies and cohesive energies the intrinsic brittleness of Ni_3Al polycrystal [6] can be understood.

COMPUTATIONAL PROCEDURE

Coincident site lattice (CSL) symmetric tilt [001] grain boundaries are generated for each of the nine tilt angles studied. For each of these boundaries, the Al can occupy one of four sublattices in each grain (top or bottom), leading to sixteen possible atomic arrangements for each boundary. However, for each boundary, there are only three unique atomic arrangements, as all others can be generated by reflection or by translations in the plane of the grain boundary. The composition of the grain boundary may be indicated by the composition of the first layer of each grain (percentage of atoms which are Ni: top grain/bottom grain): namely 100/100, 100/50, 50/50 grain boundaries. While the 100/50 grain boundary has the same stoichiometry as bulk Ni_3Al, the 100/100 boundary is Ni rich and the 50/50 grain boundary

is Al rich. (Note that some grain boundaries, not studied here, have only one possible composition e.g. [01$\bar{1}$] tilt Σ3(111).)

The generated CSL grain boundaries were relaxed to their global energy minimum using a gradient technique. Periodic boundary conditions were employed in the directions parallel to the grain boundary. At least 160 atomic layers parallel to the grain boundary were employed and the top and bottom surfaces were free. The relaxation process allowed both rigid shifts of the two grains with respect to each other as well as individual atom motion. In order to guarantee that a global energy minimum was obtained, the minimization was started at more than 10 different rigid shifts of the two grains; local minima as high as 600 mJ/m^2 above the global minimum were found.

The interactions between Ni and Al were described using potentials [9] related to those of Daw and Baskes [7]. This approach allows for a simple description of atomic interactions in the vicinity of defects such as grain boundaries and free surfaces, and has proven quite successful in a variety of applications [8]. The method is inherently many bodied and involves two distinct terms: a local density or volume term and a pairwise term. These terms are determined by fitting empirical forms to experimental data. The details of fitting the potential are described elsewhere [9]; the following is a brief summary. The pairwise interaction is taken to be a Morse potential and the density function is of the form $r^6 e^{-\xi r}$ (r is the radial distance and ξ is a parameter), leading to a total of 5 parameters using a variable distance for the (smooth) cut-off length. The shape of the embedding function [7] is chosen such that the crystal energy as a function of lattice constant matches the universal form given by Rose, et al. [10]. This leads to exact agreement with the experimental lattice constant (a_0), cohesive energy (E_{coh}), and bulk modulus. Concurrently, a best fit to the three elastic constants (two of which are independent), the vacancy formation energy (E_{vac}) and the diatomic bond length (R_e) and bond energy (D_e) is found by searching the 5 parameter space [while requiring E(fcc) < E(hcp), E(bcc)]. The RMS deviations between the calculated and experimental data in the fit are 0.8% for Ni and 3.9% for Al.

Without modifying the pure Ni and pure Al fits, a Ni-Al cross potential (Morse) is determined by optimizing a fit to the lattice parameter and cohesive energy of NiAl and Ni_3Al, as well as to the elastic constants, super intrinsic stacking fault energy (SISF), and anti-phase boundary energies of Ni_3Al and estimates of its ordering energy and vacancy formation energy. The resultant potential is capable of describing pure Ni, pure Al, diatomic Ni_2, diatomic Al_2, and Ni_3Al ($L1_2$). The energy of the (111) APB is higher than that of the (100) APB, as required for the validity of the Kear-Wilsdorf cross-slip mechanism [11] which explains the anomalous yield strength at higher temperatures.

RESULTS AND DISCUSSION

For pure Ni, pure Al and Ni_3Al, all three grain boundary types gave z-direction (perdendicular to the grain boundary) expansions of $\sim 0.1\ a_0$ relative to the perfectly symmetric starting configuration. However, the x and y shifts are different for pure Ni, pure Al and for different Ni_3Al grain boundary compositions with the same Σ. Significant rigid shifts have been observed in earlier simulations of Al by Smith, et al. [12]. The grain boundary energy (γ_{GB}) is defined as

$$\gamma_{gb} = \frac{1}{A} \sum_{i=1}^{n} \Delta E_i(\alpha_i) \qquad (1)$$

where A is the grain boundary area in our block of simulation, ΔE_i for an atom of type $\alpha(\alpha = N_i$ or Al in the present study) is

$$\Delta E_i(\alpha_i) = E_\alpha - E_\alpha^{bulk} \tag{2}$$

where E_α is the energy of this atom in the presence of grain boundary and E_α^{bulk} is the energy in the perfect alloy.

The sum in eq. (1) is over all atoms whose energy is perturbed by the proximity of the grain boundary. We find the sum converges to within 0.5 mJ/m^2 by including all atoms within 9 lattice parameters of the boundary.

We also calculated the Griffith cohesive enery of grain boundary from

$$\gamma_{coh} = \gamma_{s1} + \gamma_{s2} - \gamma_{GB} \tag{3}$$

where γ_{s1} and γ_{s2} are the energies of the two surfaces created by pulling apart the boundary. Note that even for the symmetric grain boundaries studied here, γ_{s1} and γ_{s2} may be different due to the different possible surface compositions.

The grain boundary energies are show in Fig. 1 and Table I as a function of the misorientation angle (θ), measured from the (100) plane. Also shown are the average grain boundary energies ($\langle\gamma\rangle_{gb}$) for each composition (the averages do not include $\theta = 0°$ or $\theta = 90°$). Figure 2 and Table II show the cohesive energies.

The most striking feature of these results is that γ_{GB} varies greatly with the grain boundary composition. The energy difference corresponding to the variation in composition (due to the choice of the Al sub-lattice) is from 50 to 300 mJ/m^2 for the high angle cases presented here with an average value of 156 mJ/m^2. This variation is approximately 12% of the total grain boundary energy. It is noteworthy that the 50/50 grain boundary (Al rich) has the highest γ_{GB} for each Σ, with an average grain boundary energy higher than the stoichiometric or Ni-rich boundaries by approximately 10%. We can understand this trend by noting that γ_{GB} is not always zero at tilt angles of 0° and 90°, since a perfect stoichiometry at the grain boundary is only obtained in the 100/50 case. For the $L1_2$ 100/100 composition this leads to a higher grain boundary energy of 20 mJ/m^2 and 17 mJ/m^2 for 0° and 90° respectively. The 50/50 boundaries (which are Al-rich) lead to a 617 mJ/m^2 complex stacking fault at 0° corresponding to removal of a (100) layer of 100% Ni from the perfect crystal. This introduces Al-Al nearest neighbor interactions that do not exist in the perfect $L1_2$ crystal. As the tilt angle increases from 0°, the atomic relaxations that occur can also act to lessen

Table I. Grain Boundary Energies (mJ/m^2)

θ(°)	(index)	Ni	Al	Ni_3Al		
				100/100	100/50	50/50
0	Σ1(100)	0	0	20	0	617
12.68	Σ41(540)	866	278	904	938	1054
22.62	Σ13(320)	1109	330	1101	1155	1351
28.07	Σ17(530)	1198	338	1208	1303	1388
30.51	Σ65(740)	1253	365	1305	1321	1393
36.87	Σ5(210)	1278	351	1329	1213	1396
43.60	Σ29(730)	1353	373	1417	1434	1467
46.40	Σ29(520)	1347	370	1406	1397	1484
53.13	Σ5(310)	1221	315	1166	1247	1468
61.93	Σ17(410)	1261	349	1294	1334	1407
90.00	1(110)	0	0	17	0	441
$\langle\gamma\rangle_{gb}$		1210	341	1237	1260	1379

Table II. Griffith Cohesive Energy (mJ/m^2) as defined in eq. (3)

θ(°)	(Index)	Ni	Al	Ni_3Al		
				100/100	100/50	50/50
0	Σ1(100)	3510	1710	3814	3821	3191
12.68	Σ41(540)	3206	1690	3336	3302	3186
22.62	Σ13(320)	3023	1660	3201	3146	2949
28.07	Σ17(530)	2954	1658	3104	3014	2934
30.51	Σ65(740)	2905	1633	3019	3002	2929
36.87	Σ5(210)	2886	1647	2961	3114	2968
43.60	Σ29(730)	2777	1611	2891	2881	2855
46.40	Σ29(520)	2765	1604	2904	2909	2818
53.13	Σ5(310)	2835	1635	3092	3027	2822
61.93	Σ17(410)	2699	1557	2886	2867	2815
90.00	Σ1(110)	3954	1918	4077	4119	3703
$\langle\gamma\rangle_{coh}$		2894	1663	3044	3029	2920

the severity of the Al-Al interactions. Indeed, the shift perpendicular to the grain boundary is found to be largest for the 50/50 composition, and the extra grain boundary energy due to these Al-Al interactions is reduced from 617 mJ/m^2 at 0° to an average of $\langle\gamma\rangle_{GB}(50/50) - \langle\gamma\rangle_{GB}(100/50) = 119$ mJ/m^2 for the other misorientations. The relaxed structures of Σ5(210) grain boundaries are shown in Fig. 3.

The 100/100 (Ni rich) grain boundaries are seen to have the lowest average energy, in spite of the fact that at 0° and 90°, there is a very low stacking fault energy. Also note that cusp depth of γ_{GB} in Fig. 1 varies with grain boundary composition.

Tables I and II show that the grain boundary energies in Ni_3Al (1290 mJ/m^2) are much closer to those of pure Ni (1210 mJ/m^2) than to those of either pure Al (341 mJ/m^2) or a stoichiometrically weighted average of Ni and Al (993 mJ/m^2). Furthermore, the cohesive energies of the Ni_3Al grain boundaries (~ 3000 mJ/m^2) are comparable to or higher than those of pure Ni (2894 mJ/m^2). This raises a question: If the grain boundaries in Ni and Ni_3Al are of comparable strength, why is polycrystalline Ni_3Al intrinsically brittle while Ni is ductile? The answer may lie in he plastic response of the matrix. Hack et al. have proposed a simple model for the fracture behavior of Ni_3Al [13] which can be summarized as follows. If, in a simple model of material response, failure is controlled by either plastic flow or intergranular fracture, a decrease in grain boundary cohesion at fixed yield stress or an increase in yield stress for a fixed grain boundary cohesion leads to an increased propensity toward intergranular fracture. This latter case is pertinent in the comparison of Ni_3Al to pure Ni, suggesting that Ni_3Al should show a greater tendency for intergranular fracture than pure Ni.

While recent atom probe [14] studies indicate that Ni_3Al is ordered up to the grain boundary, it is relatively insensitive to small variations in composition over a small distance. We have performed a series of simulations on the Σ5(210)/[001] grain boundary in which we exchange an Al atom from the bulk with a Ni atom from the grain boundary and visa versa. In some cases, we found that such exchanges lower the energy of the system but raise the grain boundary energy. For example, exchanging bulk Al atom with a Ni atom at a 100/50 Σ5(210) grain boundary decreases the energy of the system by 0.18 eV but raises the grain boundary energy by 453 mJ/m^2. This result suggests that real grain boundaries in Ni_3Al may not be ideally ordered and that the actual energies may be significantly higher than reported above. We are currently performing a more complete series of simulations to resolve this question.

CONCLUSIONS

We have performed atomistic simulations on nine [001] symmetric tilt grain boundaries. Depending on which sub-lattice in each of the two grains is occupied by Al, the grain boundary may have different stoichiometries. All of the simulations show that the Al-rich grain boundaries have the highest grain boundary energies. Thus Al-rich grain boundaries are more likely to fail than those which have the bulk stoichiometry or are Ni-rich. This conclusion is consistent with the observed stoichiometry dependence of the beneficial boron effect. The similarity between the grain boundary energies (cohesive energies) of Ni_3Al and Ni and the much higher yield stress of Ni_3Al provides a justification for the "inherent" brittleness of Ni_3Al grain boundaries.

ACKNOWLEDGEMENTS

This work was supported by the Energy Conversion and Utilization Technologies (ECUT) Program of the U.S. Department of Energy.

REFERENCES

[1] J. H. Westbrook, Trans. A.I.M.E. 209, 898 (1957).
[2] J. H. Westbrook, in Mechanical Properties of Intermetallic Compounds, Ed. J. H. Westbrook, Wiley, New York (1960).
[3] K. Aoki and O. Izumi, Nippon Kinsoku Gakkaishi 43, 1190 (1979).
[4] C. T. Liu, C. L. White, and J. A. Horton, Acta Metall. 33, 213 (1985).
[5] S. P. Chen, A. F. Voter, and D. J. Srolovitz, Scripta, Metall. 20, 1389 (1986).
[6] T. Ogura, S. Havada, T. Masumoto, and O. Izumi, Metall. Trans. 16A, 441 (1985); T. Takasugi, E. P. George, D. P. Pope, and O. Izumi, Scripta Metall. 19, 551 (1985).
[7] M. S. Daw and M. I. Baskes, Phys. Rev. B 29, 6443 (1984).
[8] S. Foiles, M. I. Baskes, and M. S. Daw, Phys. Rev. B, in press (1986); M. S. Daw, Surf., Sci. Lett. 166, L161 (1986); S. P. Chen, A. F. Voter and D. J. Srolovitz, Phys. Rev. Lett. 57, 1308 (1986).
[9] A. F. Voter, to be published, A. F. Voter and S. P. Chen, MRS conference proceedings, Symposium I (1986).
[10] J. H. Rose, J. R. Smith, F. Guinea, and J. Ferrante, Phys. Rev. B 29, 2963 (1984).
[11] B. H. Kear and H. G. F. Wilsdorf, Trans. A.I.M.E. 224, 382 (1962); S. Takeuchi and E. Kuramoto, Acta Metall. 21, 415 (1973).
[12] D. A. Smith, V. Vitek, and R. C. Pond, Acta Metall. 25, 475 (1977); R. C. Pond, D. A. Smith, and V. Vitek, Acta Metall. 27, 235 (1979).
[13] J. E. Hack, D. J. Srolovitz, and S. P. Chen, Scripta, Metall. (1986) in press.
[14] M. K. Miller and J. A. Hoton, (1986), preprint.

FIGURE CAPTIONS

Fig. 1 [001] tilt boundary energies as a function of misorientation angle. The dashed lines are only guides for the eye.
Fig. 2 Griffith cohesive energies as a function of misorientation angle. The dashed lines are only guides for the eye.
Fig. 3 The relaxed structures for three $\Sigma 5(210)$ boundaries. The Al and Ni atoms are represented by squares and circles, respectively; the larger symbols are closer to the reader. Extra Al-Al nearest neighbor interactions are introduced in 50/50 grain boundary (Al-rich).

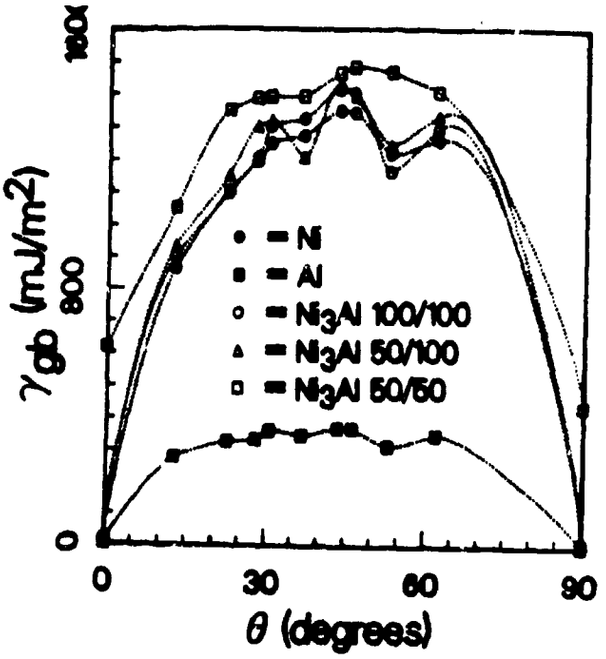

Fig. 1

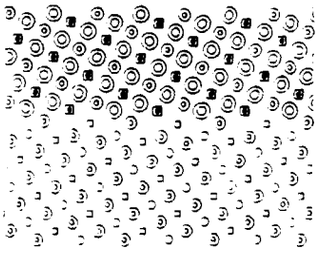

Σ5(210) (50/50)

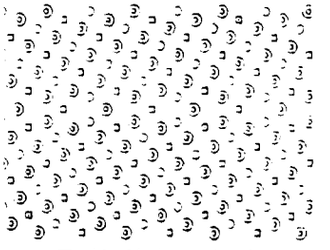

Σ5(210) (100/50)

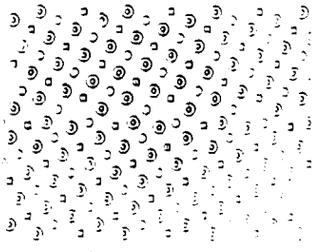

Σ5(210) (100/100)

Fig. 3

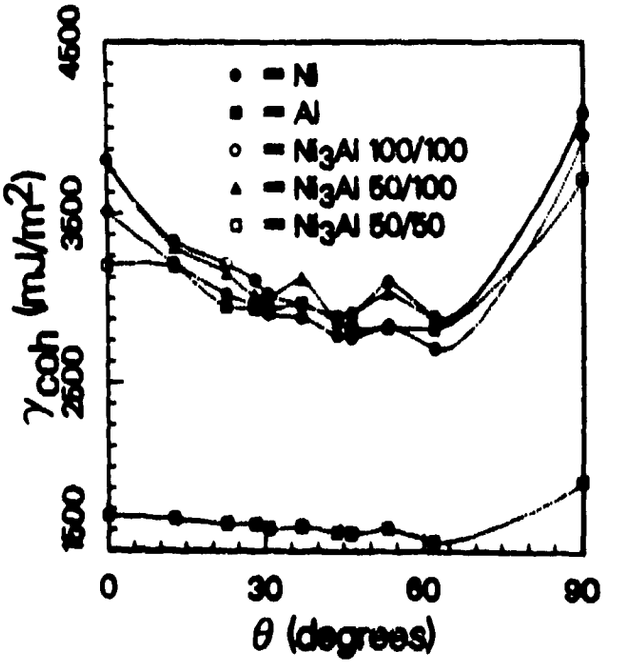

Fig. 2